FATIGUE STRENGTH REDUCTION FACTOR OF PARTIAL PENETRATION WELDMENTS FOR ITER VACUUM VESSEL

NISHI Hiroshi [1)], ETO Motokuni [2)], TACHIBANA Katsumi [1)] and NAKAHIRA Masataka [3)]

1) JAERI, Tokai Research Establishment, Tokai, Ibaraki, 319-1195, Japan

2) JAERI, Washington Office, 1825 K St., NW, Suite 508,Washington, DC 20006, USA

3) JAERI, Naka Fusion Research Establishment, Naka, Ibaraki, 311-0193, Japan

ABSTRACT

Two kinds of weldment of 316L stainless steel with artificial incomplete penetrations existed in the weld root in respect of butt and T joints were manufactured and fatigue test of the weldments was performed to investigate their fatigue behavior and the effect of the incomplete penetrations on the fatigue strength. Fatigue crack propagation test of their weld metals was also carried out using CT specimen. By calculating stress intensity factors of the weldments contained the incomplete penetrations and cracks using FEM analysis, the fatigue crack propagation rates of weldments were evaluated and compared those of their weld metals. Fatigue life of the weldments was evaluated based on fracture mechanics to discuss the effect of incomplete penetrations on the fatigue strength. As the results, the incomplete penetration behaved as a crack and most of total fatigue life for the weldment was crack propagation life. The crack propagation rates of weldment were in accordance with those of the weld metals. The fatigue strength of the weldment was considerably lower than that of smoothed specimen. The incomplete penetrations affected greatly the fatigue strength of the weldments even if the depth of incomplete penetrations was small.

INTRODUCTION

In a fusion reactor, deuterium and tritium are utilized to produce thermonuclear energy. Tritium is a radioactive material emitting β -rays and thereby must be contained securely. The high temperature plasma is confined and controlled inside a torus vacuum vessel(VV) by the magnetic force generated by the coils located outside the VV, which contains and supports in-vessel components such as the blankets and divertors. Pressure, thermal, electromagnetic and seismic loads are expected to be imposed on the reactor components independently or simultaneously. Therefore, the VV is the most important component in view of the fact that it is the first barrier to prevent tritium release from the reactor. As for the VV, ductile fracture caused by the pressure, electromagnetic and seismic loads, low cycle fatigue caused by the cyclic electromagnetic and thermal stresses, and excessive plastic deformation due to the combination of such primary and cyclic thermal stresses are identified to be the dominant failure modes [1,2].

The vacuum vessel of ITER is designed adopting 316LN (0.06-0.08% nitrogen) stainless steel double-walled structure and composed of inner and outer shells, 40-60 mm in thickness, jointed by welded stiffening ribs [3]. It is also divided toroidally into sectors, which are jointed by field welding at the central plane of ports, and filled with shielding plates between the inner and outer shells to prevent from neutron. Therefore, many kinds of welding are employed in the VV. However, some weldments are not full penetration joints, which are not qualified in the conventional design standards for light water reactor. It is also crucial to develop the integrity evaluation method for the weldments based on proper structural design code. Namely, weld joint efficiency and fatigue strength reduction factor for primary stress should be developed. The sufficient data on mechanical properties of the weldments are required to establish new structural design guideline for ITER VV. Therefore, the evaluation of the effect of weld defects on the fatigue strength is one of most important problem from view points of fatigue design and quality control procedures related to welded structures.

In this study, fatigue behavior of the weldments with incomplete penetration(IP) was investigated, because only few data are available for the effect of the IP on fatigue strength of weldments[4-7]. Two kinds of weldment with artificial IP existed in the weld root were manufactured, which are candidate welding processes for the fabrication of ITER VV. One weldment was a butt joint using tungsten inert

gas(TIG) welding in the light of field welding of the initial assembly of VV. The other weldment was square T joint, which is employed for connection between the outer shell and rib, using metal active gas(MAG) welding after TIG welding for a root pass. Fatigue test of the weldments were performed using as-welded large specimen to explore their fatigue crack propagation and fatigue strength. Fatigue crack propagation test of their weld metals was also carried out using CT specimen. By calculating stress intensity factors of the weldments contained the incomplete penetrations and cracks using finite element method (FEM), the fatigue crack propagation rates of weldments were evaluated to compare those of their weld metal. Moreover, fatigue life of the weldments were evaluated based on fracture mechanics to discuss the effect of the depth of IP on their fatigue strength in the light of fatigue strength reduction factor.

EXPERIMENTAL PROCEDURE

Material and Welding Procedure

A plate of 40mm thick 316L stainless steel was employed in this study. Chemical compositions of the 316L stainless steel and filler metals used for the welding are listed in Table1. In this study, two kinds of weldment were fabricated by TIG and MAG welding processes and their combinations. Their welding procedures are summarized in Table2 and their microstructures are shown in Fig.1. One weldment was one side welding of butt joint using narrow-gap TIG welding with the IP existed in the weld root. The depth of IP was approximately 3 mm without root opening gap as shown in Fig.1(a). The weld reinforcement was removed by grinding. Another weldment was T joint which is employed for connection between the outer shell and rib. The T joint was welded by the MAG welding after the TIG welding for a root pass and included incomplete penetrations at the both side root faces without root opening gap as shown in Fig.1(b). The depths of left and right side IP were approximately 6.8 mm and 7.7 mm respectively. In these welding procedures, the IP were artificial defects and are possible to reduce their depths in the fabrication of VV. Mechanical properties of weld metals for the weldments are listed in Table3 being compared with that of 316 stainless steel base metal. Both weld metals had sufficient strength rather than the base stainless steel. As for the T joint, a cruciform joint was manufactured by welding an additional 40 mm thickness plate to the T joint in order to obtain tensile fatigue specimen as shown in Fig.2. Both weldments were prepared for the size 1000mm width and 600mm length.

Table1 Chemical compositions of 316 stainless steel and filler metals.

Materials	C	Ni	Cr	Mo	Mn	Si	P	S
316L SS	0.011	12.07	17.16	2.14	1.07	0.51	0.021	0.001
Filler Y316L	0.018	12.23	19.32	2.3	1.98	0.47	0.022	0.002
Filler YF316LC	0.031	11.72	18.87	2.5	1.16	0.62	0.024	0.005

Table2 Welding processes and conditions.

Butt joint		T joint	
Groove and welding process	Welding conditions	Groove and welding process	Welding conditions
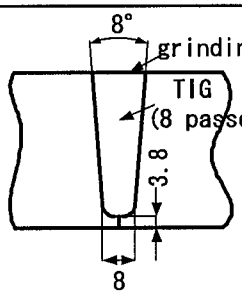	TIG welding Current 180-375A Voltage 13-18.5V Speed 70-555mm/min Filler: Y316L	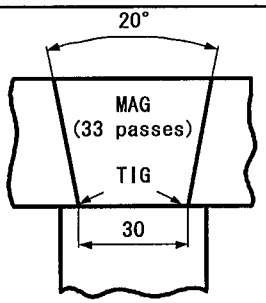	TIG welding 160-170A 17V 120mm/min Filler:Y316L MAG welding 270-300A 30-32V 320-430mm/min Filler:YF316LC

Table3 Mechanical properties of 316L SS and weld metals.

Materials	0.2 % proof stress (MPa)	Tensile strength (MPa)	Elongation (%)
316L SS Base	245	557	68
weld metal of MAG	436	590	44
weld metal of TIG	430	610	45

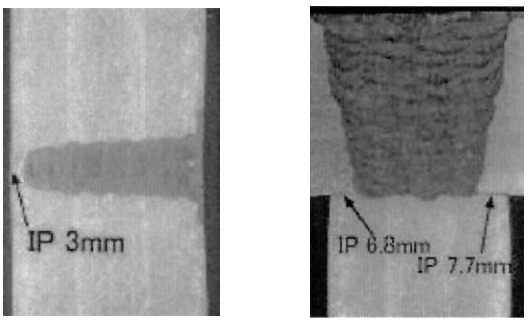

(a) Butt joint (b) T joint

Fig.1 View of macro-structure of weldments.

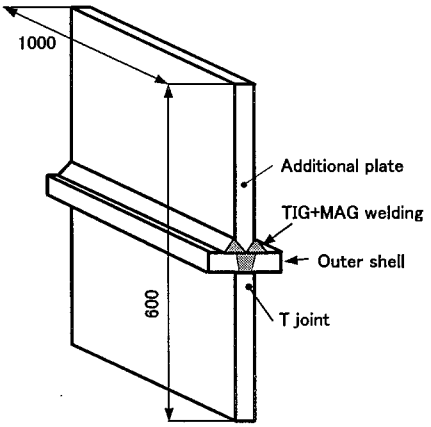

Fig.2 Configuration of T joint(mm).

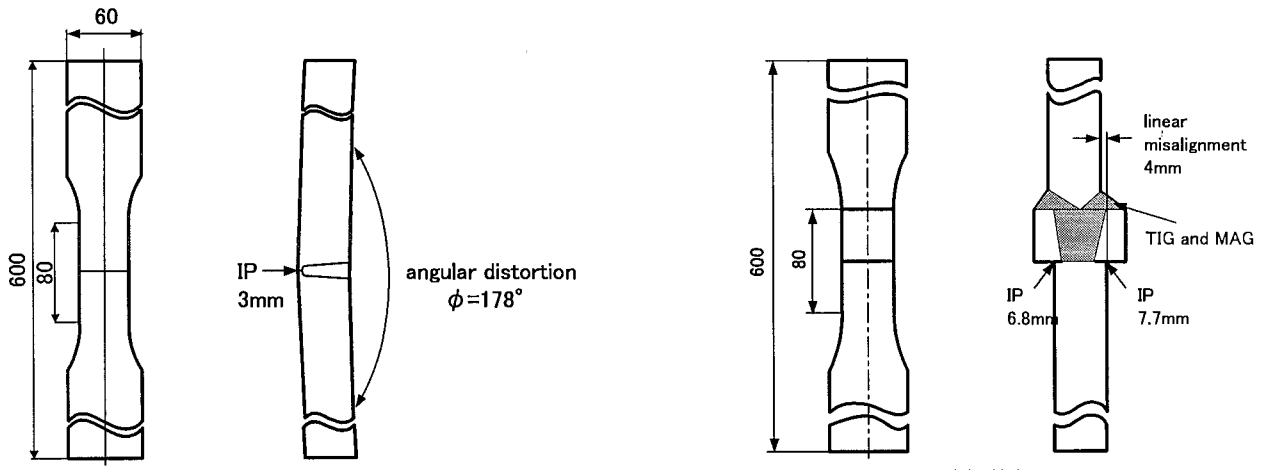

(a) butt joint (b) T joint

Fig.3 Configuration of fatigue specimens of weldments (mm).

Fatigue Test

Fatigue test was carried out using as-welded large specimens, which were machined with the IP located at its center as shown in Fig.3. The weldment of butt joint had an angular distortion at angle 178° caused by welding distortion as shown in Fig3(a). On the other hand, a linear misalignment of 4 mm was occurred in the case of T joint. The fatigue test was performed at room temperature using a hydraulic fatigue machine of load capacity 490 kN by clamping the specimen with hydraulic grips. Tensile loads with stress ratio R=0 were controlled at frequency 0.5Hz. Crack growth was also monitored with taking photos of cracks during the fatigue test in order to obtain fatigue crack propagation rates of the weldments. Since the estimated stress cycles caused by electromagnetic force concerned with the VV are not exceeding $5x10^4$ cycles, the applied stress levels were determined to make the fatigue life less than 10^5 cycles. In addition to the fatigue test of large specimens for the weldments, fatigue crack propagation test of their weld metals using CT specimen (13 mm thick)was carried out with stress ratio R=0.05 and frequency 10Hz to compare the crack propagation rates of the weldments.

Stress Analyses of Weldment Using FEM

As mentioned above, the weldments contained the IP in weld root, which was a slit without opening gap like a crack. In general, fatigue cracks initiate from the discontinuities such as the IP associated with the weldment. In order to evaluate crack propagation rates in engineering structures, stress intensity factor range, ΔK, is widely used. In this study, ΔK was used as a correlation parameter of the fatigue crack propagation rates. In order to calculate ΔK at various crack lengths for the weldments, FEM analysis were conducted taking account for the angular distortion of the butt joint and for the linear misalignment of the cruciform joint, in which the IP was regarded as a crack. Models used in the analysis were sections of the specimens as shown in Fig.4(a) and (b) for the butt joint and T joint respectively. The specimens were loaded by uniform tensile displacement applied to their top nodes. Figure 5 shows used meshes for the butt joint and T joint. In the case of the butt joint, the mesh was divided in only a top half of the model because of axial symmetry of its deformation, while the mesh was whole of the model for the T joint. Both models were plain strain condition and adopted singularity elements to the crack tips. The analysis used the FEM code of ABAQUS with 8-node isoparametric quadrilateral elements with the same elastic modulus E=192GPa and Poisson's ratio ν=0.3 for the weld metals and base steel.

Since the results of the analysis indicated the cracks were subjected to mode I loading for both joints, J integral, J, around the crack tips calculated by the FEM analysis and converted to stress intensity factor, K, using Eq. (1)

$$K = \sqrt{\frac{E \cdot J}{1-\nu^2}} \tag{1}$$

As for the T joint, the K were calculated from the J integrals for the both side cracks.

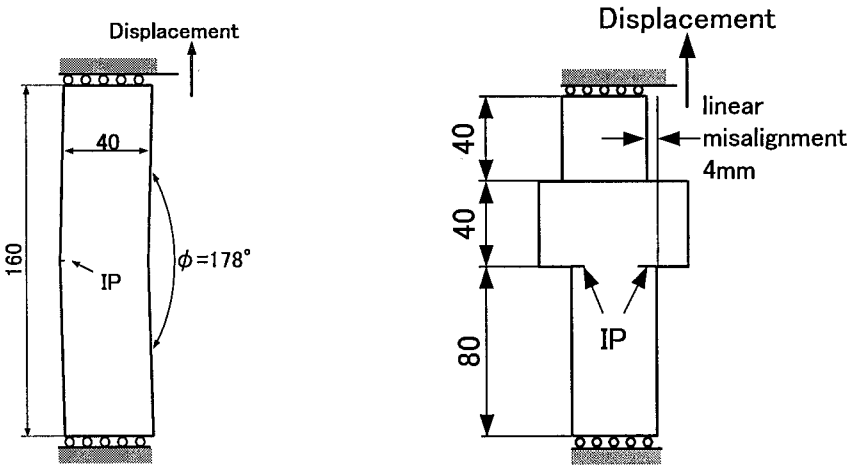

(a) Butt joint (b) T joint

Fig.4 FEM analysis models.

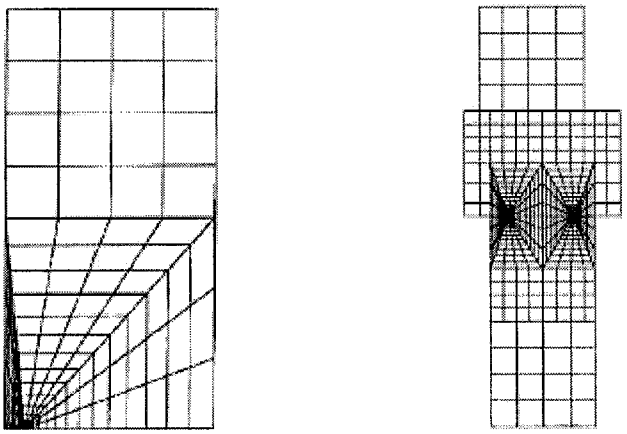

(a) Butt joint (b) T joint

Fig.5 Meshes used for FEM analysis.

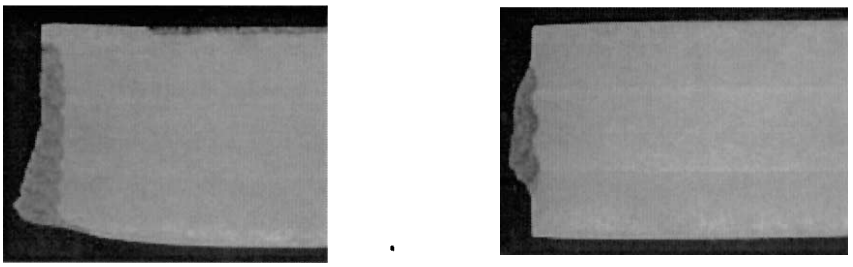

(a) Butt joint (b) T joint

Fig.6 Cross sectional views of fracture large specimen

RESULTS AND DISCUSSION

Crack Propagation Behavior

Figure 6 exhibits cross sectional views of the failure specimens. All fatigue specimens fractured at the IP and the cracks propagated through the weld metal perpendicularly to the loading direction. Crack propagation curves are shown in Fig.7(a) and (b) , in which the length of both side cracks are exhibited in the case of T joint. When the crack initiation was defined as 0.1 mm of crack growth from the tip of IP, ratios of the crack initiation life to the total fatigue life were less than 3% for both joints. Namely, most of total fatigue life was crack propagation life. Since the tip of IP was very sharp without root opening gap, the IP behaved and propagated like a crack. As for the T joint, the crack propagated almost from the left side IP because of the large stress intensity factor range as explained next section.

Stress Intensity Factor By FEM Analyses

Figure8 shows the results of stress intensity factor divided by applied stress(nominal stress), K/σ , at the maximum load obtained by FEM analysis. The K/σ around the crack tip was tensile stress condition for the butt joint, though the specimen applied bending moment caused by the angular distortion. As for the T joint, the K/σ for both side cracks were evaluated and the abscissa i.e. the crack length designated the crack length of left side crack. The K/σ of right side crack was smaller than that of left side crack owing to the bending moment caused by the linear misalignment, though the depth of the right side crack was larger than that of left side crack. The K/σ of right

side crack gradually decreased with increasing the depth of left side crack. The fit curves of K/ σ for the butt and T joints as shown in Fig.8 were obtained by the least square analysis as following polynomial expressions.

$$K/\sigma = 0.0734 + 15.42 \times a - 180 \times a^2 + 13070 \times a^3 \quad \text{for butt joint} \tag{2}$$

$$K/\sigma = 0.1038 + 12.85 \times a + 227 \times a^2 + 285 \times a^3 \quad \text{for butt joint} \tag{3}$$

where a is the depth of crack or left side crack(mm).

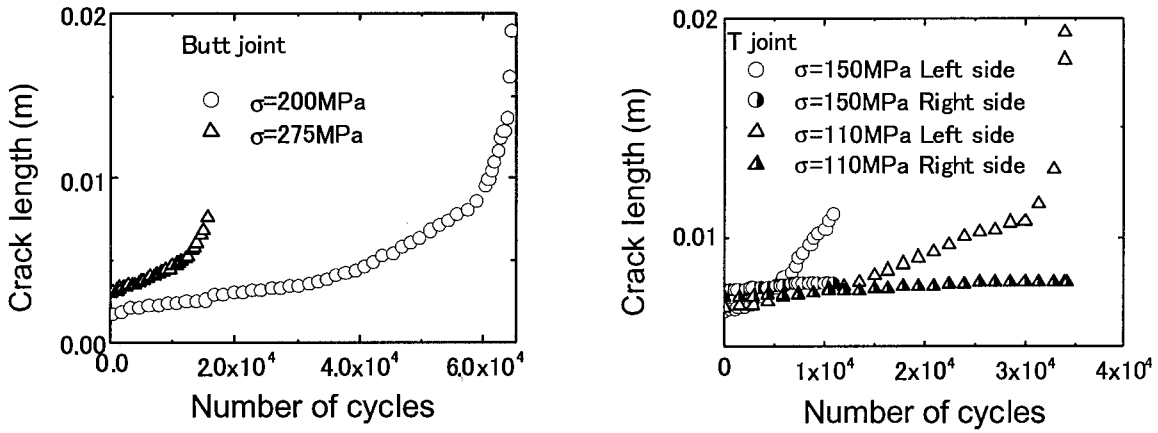

(a) Butt joint (b) T joint

Fig.7 Crack propagation curves of weldments.

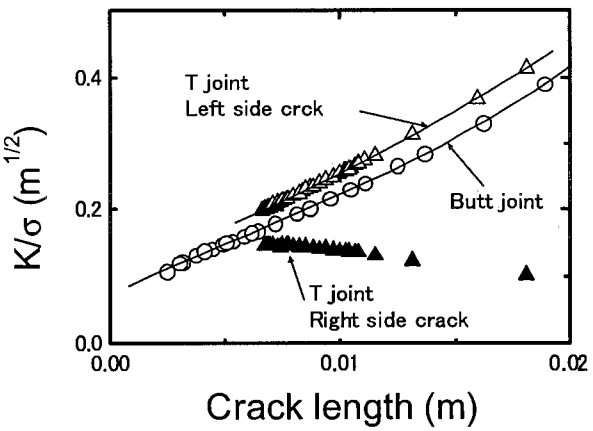

Fig.8 Stress intensity factors obtained by FEM.

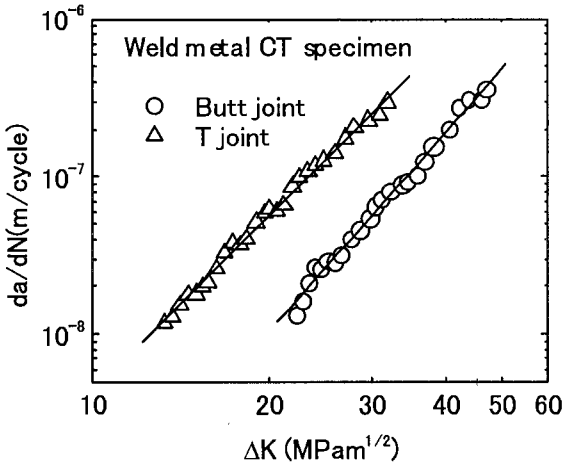

Fig.9 Crack propagation rates for weld metals.

Crack Propagation Rate

The results of crack propagation rates, da/dN, of the weld metal for the butt and T joints using CT specimen are shown in Fig.9 as functions of stress intensity factor range, ΔK. The da/dN of T joint weld metal were about 5 times as large as those of the butt joint. The degradation related to T joint is attributed to its microstructure of the weld metal because of the MAG welding.

The crack propagation rates, da/dN, of the weldments versus ΔK evaluated by FEM analysis, are shown in Fig.10(a) and (b) for the

butt and T joint, respectively. In this figures, the da/dN of the weld metals are also indicated to compare with those of the weldments. As for the butt joint, the da/dN of the weldment were large rather than those of the weld metal. It is considered that the increase of da/dN is attributed to the residual stress of weldment. For the T joint, however, the da/dN of the weldment were corresponding to those of the weld metal for both side cracks, while the ΔK and the depths of right side cracks were smaller than those of the left side cracks. The fit lines obtained by the least squares analysis for the da/dN of weldments shown in Fig.10 can be expressed as follows.

$$da/dN = 1.10\times10^{-13}\Delta K^{4.08} \qquad \text{for butt joint} \tag{4}$$

$$da/dN = 1.26\times10^{-13}\Delta K^{4.30} \qquad \text{for T joint} \tag{5}$$

Fatigue Strength

The fatigue strength of the weldments is shown in Fig.11 making comparison with that of smoothed steel, which was so-called best-fit curve obtained by Langer [8]. The fatigue life, N_f, was defined as the number of cycles to the complete failure. The fatigue strength of the weldment was extremely lower than that of smoothed specimen and fatigue strength reduction factor K_f was approximately 5 and 11 for the butt and T joints respectively.

In order to evaluate fatigue life of the weldments and the effect of IP on the fatigue strength, the fatigue life of weldments were analyzed based on fracture mechanics. Integrations of Eq.(4) and (5) were numerically conducted from the initial crack length i.e. the depth of IP to the final crack length substituting the Eq.(2) and (3) respectively, which were the relations between K and crack length obtained by the FEM analysis. The calculation was performed not only for the specimen used for the fatigue test but also for the specimen contained IP of 1 mm depth for the butt and T joints. These results are also designated in Fig.11. The evaluated fatigue life for the used fatigue specimens was corresponding to the experimental fatigue life. So the fatigue life could be predicted based on the fracture mechanics. As for the specimen contained IP of 1 mm depth, the fatigue strength reduction factor $K_f$was about 4 and 7 for the butt and T joints respectively, while the fatigue life were several times as long as those of the fatigue specimens. The fatigue strength of weldment with the IP was extremely decreased against the smoothed specimen even if the depth of IP became small. Namely, the IP of weldments affected greatly their fatigue strength.

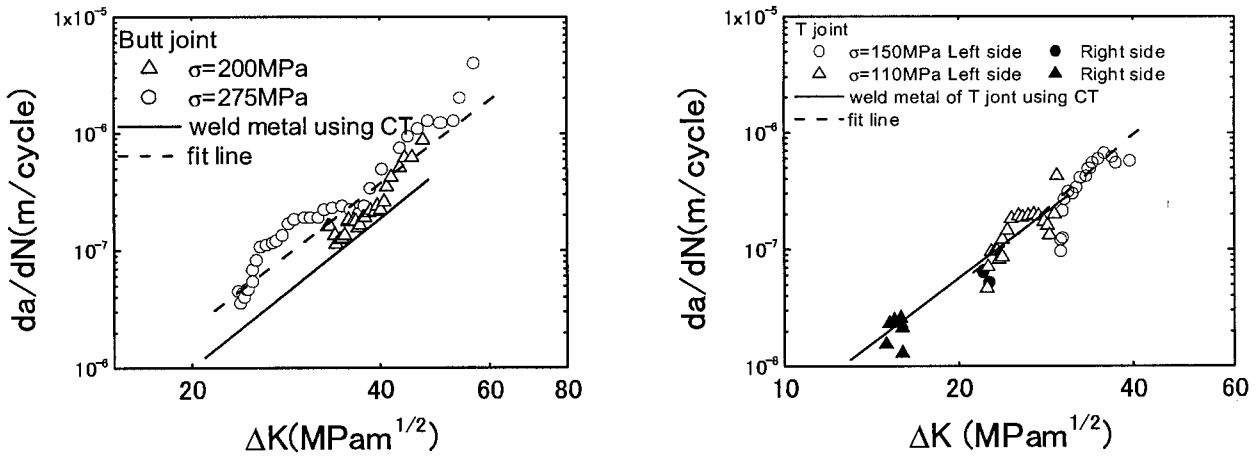

(a) Butt joint (b) T joint

Fig.10 Crack propagation rates of weldments making comparison with those of weld metals.

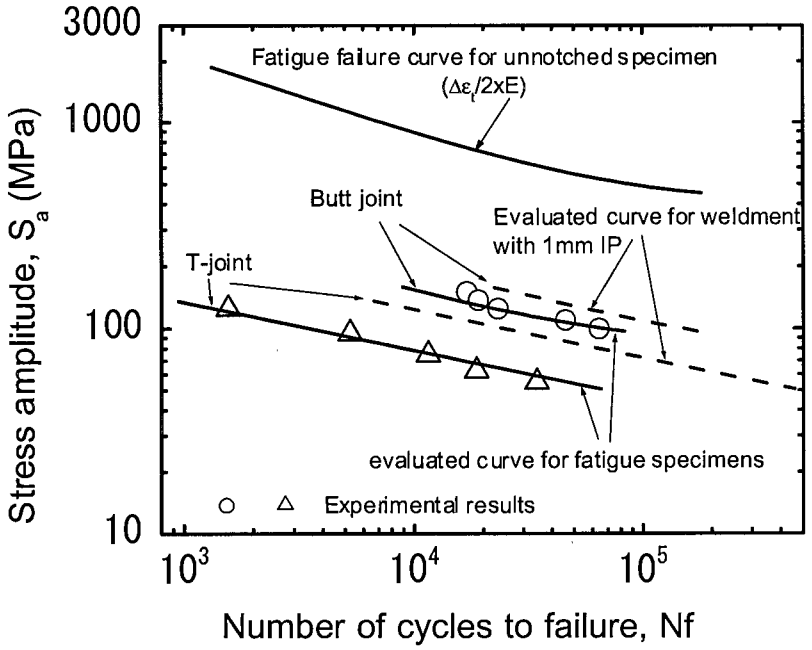

Fig.11 Fatigue strength of weldments compared with those of smoothed specimen and evaluated fatigue strength based on fracture mechanics.

CONCLUSIONS

Two kinds of weldment of 316L stainless steel with artificial IP existed in the weld root were manufactured and fatigue test of the weldments was carried out to investigate their fatigue behavior and the effect of the IP on the fatigue strength. By calculating stress intensity factors of the weldments contained the IP and cracks, the fatigue crack propagation rates of weldments were evaluated and compared those of their weld metals. The fatigue life of the weldments were evaluated based on fracture mechanics to investigate the effect of depth of the IP on fatigue. Conclusions may be summarized as follows:

(1) The IP behaved and propagated as a crack and most of fatigue life for the weldment was crack propagation life.

(2) The crack propagation rates of weldments were in accordance with those of the weld metal.

(3) The fatigue life could be predicted based on the fracture mechanics.

(4) The fatigue strength of the weldments with the IP was considerably lower than that of smoothed specimen. The IP of weldments affected greatly their fatigue strength even if the depth of IP was small.

REFERENCES

1. K. Miya, et al., Fusion Engineering &Design, 31, pp.145-165 (1996).
2. K. Miya, et al., Fusion Engineering &Design, 41, pp.305-312(1998).
3. K. Koizumi, et al., Fusion Engineering &Design, 41, pp.299-304(1998).
4. Y. Ishii, H. Kihara and Y. Tada, J. Japanese Society Non-Destructive Inspection, 16, pp.319-345(1967).
5. R. F. Ashton, R.P. Wesley and C.R. Dixon, Welding Research Supplement, 54, pp.95s-98s(1975).
6. S. J. Maddox and D. Webber, ASTM STP 648, pp.159-184(1978)
7. M.Higuchi, et al., PVP-Vol.313-1, International Pressure Vessel and Piping Codes and Standards : Volume 1, pp.69-76(1995)